First-principles investigation of the stability of MN and CrMN precipitates under coherency strains in α-Fe (M = V, Nb, Ta)

Dan H. R. Fors[a] and Göran Wahnström
Department of Applied Physics, Chalmers University of Technology, SE-412 96 Göteborg, Sweden

(Received 7 January 2011; accepted 19 February 2011; published online 7 June 2011)

We perform a systematic *ab initio* study of the interface energetics of thin coherent rocksalt (nacl) structured MN and tetragonal CrMN films in bcc Fe (M = V, Nb, Ta), motivated by the vital role of MN and CrMN precipitates for the long-term creep resistance in 9%–12%Cr steels. The similarities and differences in the work of separations and the elastic costs for the coherency strains are identified, and the possibility for formation of coherent films are discussed. Our findings provide valuable information of the interface energetics, which in continuation can be combined with thermodynamical modeling to obtain a better understanding of the initial nucleation stage of the MN and CrMN precipitates, and their influence on the long-term microstructural evolution in 9%–12%Cr steels. © *2011 American Institute of Physics*. [doi:10.1063/1.3573392]

I. INTRODUCTION

Martensitic 9%–12%Cr steel alloys are widely used today for components in fossil-fired steam power plants with steam temperatures up to 600 °C, where excellent creep properties and sound oxidation protection are required.[1] Their strength and long-term creep resistance rely strongly on a fine-grained martensitic microstructure, Cr-rich $M_{23}C_6$ (M = Fe, Cr) carbides, and dispersion strengthening by densely distributed MN (M = V, Nb, Ta) precipitates, which together effectively restrict migration of dislocations and subgrain boundaries under service. In particular, the MN precipitates have a very important role for the creep strength due to their high number density and extremely slow coarsening rate.[2,3] However, after long-term exposure at elevated temperatures (600-650 °C), the 9%–12%Cr steels have been discovered to experience premature breakdown due to the precipitation of a complex nitride phase known as Z-phase, CrMN (M = V, Nb, Ta).[4,5] The Z-phase nucleates and grows large coarse platelets on the expense of the finely distributed MN phase,[4–7] which leads to a decreased dispersion strengthening and to a detrimental reduction of the creep strength.[5] The discovery has initiated intense research with the aim to either suppress the Z-phase nucleation during the entire lifetime of components or alternatively to accelerate the nucleation process to such an extent that the Z-phase can be utilized for dispersion strengthening.[5,8,9]

The Z-phase has, from experimental observations, been found to be more thermodynamically stable than the MN phase in the creep service temperature range 600–700 °C,[5,10] which has also been supported by thermodynamical modeling.[8,11,12] Yet, the Z-phase has surprisingly never been found to nucleate on its own, despite that the only difference in composition compared to the MN phase is Cr, which is abundant in the alloy.[9] Instead, the Z-phase nucleation occurs slowly through a continuous process where metastable precursors are created by Cr diffusion into pre-existing MN precipitates. The precursors are then subsequently gradually transformed into the Z-phase by internal atomic rearrangements.[5,10,13,14] The apparent difficulty for direct nucleation has been suggested to be attributed to a significantly lower probability for compositional fluctuations to form a nucleus of the complex Z-phase (or Z-phase-like) structure compared to a nucleus of the MN phase,[11,15] or alternatively to a higher interface energy for the Z-phase, which according to classical nucleation theory would give a substantially higher nucleation barrier.[14,16]

The importance of the interface energetics for the nucleation stage is supported by experimental observations,[17] which have shown that the (V,Nb)N precipitates nucleate as thin coherent platelets in steel alloys. These platelets suggest that the corresponding interface energies are very small, which opens up for the possibility that the Z-phase compounds could have a higher interface energy. A fundamental understanding of the interface energetics of the MN and Z-phase precipitates is therefore an important area for investigation as a step toward finding an explanation for the nucleation difficulty of the Z-phase.

In the present paper we perform a systematic investigation of the coherent interface energetics of nacl-structured MN and tetragonal CrMN precipitates in bcc Fe. The coherent interfaces are treated with density functional theory (DFT) calculations, which in previous theoretical studies[18–34] have proven to be a powerful and an accurate tool to describe the electronic structure at metal–ceramic interfaces. Our results provide valuable information about the similarities and differences in the interface energetics of the MN and CrMN phases, which in continuation can be combined with thermodynamical modeling[8,12] to obtain a better understanding of the initial nucleation stage of the MN and Z-phase precipitates in 9%–12%Cr steel alloys.

The paper is organized as follows. First, the methodology to treat the coherent interfaces is presented in Sec. II. Then, in Sec. III the computational techniques for the atomistic calculations are described followed by the results

[a]Author to whom correspondence should be addressed. Electronic mail: forsdan@chalmers.se.

(Sec. IV) and discussion (Sec. V). The main conclusions of our study are summarized in Sec. VI.

II. METHODOLOGY

In this paper we focus on thin plate-like precipitates which are defined by two sharp interfaces and a thickness h of the slab. The precipitates are assumed to have an infinite extension in the parallel direction to the interface and hence, effects such as mismatch at the sides of a real finite precipitate are neglected. Further, the surrounding Fe phase is assumed to have an infinite extension, and all coherency strains are thus taken up by the nitride phase.

The orientation relationship for the interfaces is adopted to the so-called Baker–Nutting relationship, i.e., $(001)_{\mathrm{nacl}} \,||\, (001)_{\mathrm{bcc}}, [100]_{\mathrm{nacl}} \,||\, [110]_{\mathrm{bcc}}$ for the Fe|MN interfaces, and $(001)_{\mathrm{Z}} \,||\, (001)_{\mathrm{bcc}}$, $[100]_{\mathrm{Z}} \,||\, [100]_{\mathrm{bcc}}$ for the Fe|CrMN interfaces. This orientation relationship has been experimentally established for VN,[37] (V,Nb)N,[4] NbN,[38,39] and Cr(V,Nb)N (Ref. 40) precipitates, whereas for TaN, CrNbN, and CrTaN no data are currently available. However, in order to allow for a consistent investigation of the interface energetics we adopt the Baker–Nutting relation for all compounds.

We decompose the total interface energy E_{tot} into two terms,

$$E_{\mathrm{tot}} = E_{\mathrm{el}} + E_{\mathrm{chem}}, \tag{1}$$

where E_{el} describes the elastic costs associated with the coherency strains of the nitride phase, and E_{chem} the chemical energy originating from the breaking and creation of bonds in the interface formation. The former will depend on the size of the lattice misfit f and increase linearly with the slab thickness, $E_{\mathrm{el}} \propto hf^2$.

III. COMPUTATIONAL DETAILS

The calculations are performed within the framework of DFT as implemented in the Vienna *ab initio* simulation package (VASP).[43–45] Blöchl's all-electron (frozen core) projector-augumented-wave formalism (PAW) as implemented by Kresse and Joubert[46] is employed for the electron–ion interaction, where the standard Fe, Cr, V, Nb, Ta, and N potentials with 14, 12, 11, 11, 11, and 5 valence electrons, respectively, are used. For Fe it is well-known that spin–polarized generalized gradient approximations (GGAs) for the electron exchange-correlation (xc) functional are needed to give an accurate description of its structural, energetic, and magnetic properties.[47] The xc-functional is therefore here treated with the spin–polarized GGA according to Perdew, Burke, and Ernzerhof (PBE),[48] which in previous comparisons between semilocal functionals has shown to provide the best overall description of the bulk properties of 3*d* transition metals, in particular of Fe, and a good account of the bulk properties of 4*d* and 5*d* transition metals.[49,50]

The k-point integration over the Brillouin zone is performed by using a Monkhorst–Pack grid and the first order Methfessel-Paxton smearing scheme, where the fictitious temperature broadening is set to 0.1 eV in order to allow for an accurate extrapolation to $T = 0$ K. The plane-wave energy cutoff 700 eV is used in all calculations to ensure that the absolute total energies are converged within 1 meV/atom. The equilibrium volumes and cell shapes of the compounds are optimized by minimizing the stress tensor components, whereas the internal structural parameters are fully relaxed by using a conjugate-gradient algorithm until the Hellman–Feynman forces acting on each atom are less than 0.02 eV/Å.

The similarities and differences in the electronic structure for the considered systems are studied in terms of atom-projected density of states (DOSs) and charge transfers between different constituents. The charge transfers are quantified through Bader analysis[51] based on the approach given in Ref. 52. The Bader scheme represents an intuitive way to separate atoms from each other in compounds, based solely on the charge density, and can provide value information about charge redistributions. The evaluation of the DOSs are also carried out within the Bader volumes by using a tool to VASP developed by Tang and Henkelman,[53] which allows the entire electron charge density to be projected onto the atoms.

A. Bulk properties

The bulk calculations are performed by using a two-atom unit cell for bcc Fe, a four-atom unit cell for the nacl MN systems, and a six-atom unit cell for the tetragonal CrMN compounds (cf. Fig. 1). The converged k-point grids are set to $12 \times 12 \times 12$, $12 \times 12 \times 12$, and $12 \times 12 \times 6$, respectively. Ideal stoichiometry is assumed for all structures, and thus the presence of nonmetal vacancies, which experimentally are known to stabilize the MN phases, are omitted in order to reduce the number of varying parameters.

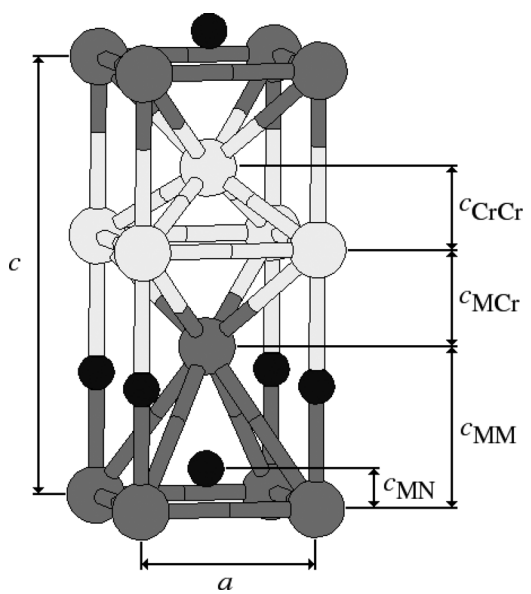

FIG. 1. Lattice structure of the tetragonal CrMN phase (Z-phase) (Refs. 5, 35, and 36). The white, gray, and black spheres denote the Cr, M, and N atoms, respectively. Further, c_{AB} denotes the interlayer distance between (001) planes consisting of A and B atoms.

B. Interface properties

The coherent interface systems are represented by using a computational unit cell containing a standard slab geometry with n_{Fe} Fe layers on top of n_N coherently strained nitride layers, where the interlayer distances perpendicular to the interface in the nitride phase are adjusted to account for the Poisson relaxation. Each MN layer contains one M atom and one N atom, whereas each Fe and Cr layer corresponds to one Fe and one Cr atom, respectively. The cell is subjected to periodic boundary conditions in all three directions. The relative translation of the two phases is chosen so that the Fe atoms are on top of the N atoms, which has been shown to be the optimal configuration for the Fe|MN interfaces.[18,21,34] The converged k-point grids are set to $12 \times 12 \times 1$.

At $T = 0$ K the chemical contribution to the interface energy can be evaluated according to

$$E_{chem} = \frac{E - \sum_i \mu_i N_i}{2A}, \tag{2}$$

where A is the area, N_i the number of atoms for the constituent i, and E is the internal energy of the interface system. The factor 2 in the denominator is included to account for the presence of two interfaces in the computational unit cell. The chemical potentials μ_i are evaluated under the assumption that each interface is in equilibrium with the bulk bcc Fe phase and the strained nitride compound. For the Fe|CrMN interface systems, this choice of the reference states restricts the number of layers n_N to multiples of four. Consequently, three different interface terminations become possible, which we denote by $Z_{MN-MN-Cr-Cr}$, $Z_{MN-Cr-Cr-MN}$, and $Z_{Cr-MN-MN-Cr}$, respectively, where the jth subindex corresponds to the jth interface layer. For the $Z_{MN-MN-Cr-Cr}$ termination, the two interfaces in the computational unit cell are not identical to each other, and hence, throughout this work we will present the average of the two interface energies in this case.

Further, atomic relaxation along the z-axis at the interface is permitted for the Fe and the CrMN phases, whereas for the MN phases the interlayer distances are kept fixed. This constraint is imposed as a consequence of the dynamical instabilities along the X and K high symmetry points found for the stoichiometric nacl-structured VN, NbN, and TaN compounds.[54–56] These instabilities introduce large shear displacements in the nacl-structure, which are stabilized first when nitrogen vacancies are introduced. The implications from omitting the atomic relaxation of the MN phases are discussed in Sec. V A.

Convergence tests with respect to the number of layers show that $n_{Fe} = 9$ is sufficient to reduce the interface energy error arising from the artificial interface interactions through the Fe phase to less than 0.01 J/m^2. Based on these convergence results, the interface energy calculations are performed by using $n_{Fe} = 9(10)$ in combination with n_N equal to an odd (even) number of layers.

The absolute bond strength of the interface systems is analyzed is terms of the work of separation

$$W_{sep} = \sigma_{Fe} + \sigma_N - E_{chem}, \tag{3}$$

where σ_{Fe} and σ_N denote the surface energy of the free Fe surface and the strained nitride surface, respectively. The surface energy σ is for each phase calculated according to

$$\sigma(n) = \frac{E_{surf}(n) - \sum_i \mu_i N_i}{2A}, \tag{4}$$

where $E_{surf}(n)$ is the internal energy of a surface system represented by a standard slab geometry with n layers and a 12-Å-thick vacuum region. Convergence tests show that $n_{Fe} = 16$ and $n_N = 16$ are sufficient to reduce the surface energy errors to less than 0.02 J/m^2.

Finally, the surface energies are also used to evaluate the intrinsic work of separation in each bulk phase according to

$$\bar{W}_{sep} = 2\sigma, \tag{5}$$

which reflects the absolute strength of the internal bonds.

IV. RESULTS

A. Bulk properties

In Table I we present the bulk properties as calculated with DFT together with experimental data for bcc Fe, nacl MN, and tetragonal CrMN. The magnetic structure at the equilibrium volume is determined to be ferromagnetic for Fe and nonmagnetic for the nitrides.

For VN, we find that GGA–PBE gives a very accurate account of the lattice parameter, whereas for Fe, NbN, and TaN the relative differences are larger (−1.0%, 1.8%, and 2.1%, respectively). For NbN and TaN, it is however important to note that a direct comparison with experimental data should be done with caution, as the compounds, in general, are substoichiometric with varying amounts of nitrogen vacancies. It is known that such defects can have an effect on the lattice parameter of the material.

For the CrMN phases the calculated structural parameters are found to be in reasonable agreement with the measured structural data, apart from a deviation of the internal buckling c_{MN} in CrNbN and the c lattice parameter of CrVN. However, it should be noted that the experimental measurements are performed at finite temperatures, in contrast to the DFT calculations, which are performed at 0 K, which can give rise to thermal expansion and changes of the interlayer distances. Such effects have not been accounted for in this study. In addition for the CrVN phase the discrepancy may be due to the finite Nb content in Cr(V,Nb)N, or alternatively, due to the very long transformation time of the (V,Nb)N phase into the Cr(V,Nb)N compound.[5] The latter could lead to the fact that the experimental values of the Cr(V,Nb)N phase are measured on precursor states to the stable tetragonal phase. A more thorough study, exploring alternative structures, would be needed though to resolve the origin of this discrepancy.

Further, for CrVN and CrNbN, we are aware of two theoretical studies of the structural parameters,[11,12] obtained with DFT–PAW and the xc-functional according to Perdew and Wang[57] (PW91), cf. Table I. Our calculated results are in qualitative agreement with the cell parameters in Refs. 11

TABLE I. Lattice parameters (a, c), interlayer distances c_{AB} between planes consisting of A and B atoms (cf. Fig. 1), magnetic moments (m), and Bader charge transfer from the M to the N atoms (Bader) for the investigated bulk phases.

Method	System	a (Å)[a]	c (Å)	c_{MM} (Å)	c_{MCr} (Å)	c_{CrCr} (Å)	c_{MN} (Å)	m (μ_B)	Bader[b] ($\|e\|$)
DFT–PBE[c]	Fe	2.8385	···	···	···	···	···	2.20	···
Experiment	Fe	2.866	···	···	···	···	···	2.22	···
DFT–PBE[c]	VN	2.917	···	2.063	···	···	···	0.0	1.62
	NbN	3.151	···	2.228	···	···	···	0.0	1.73
	TaN	3.130	···	2.213	···	···	···	0.0	1.86
Experiment	VN[d]	2.918	···	2.063	···	···	···	···	···
	NbN[e]	3.096	···	2.190	···	···	···	···	···
	TaN[d]	3.066	···	2.168	···	···	···	···	···
DFT–PBE[c]	CrVN	2.862	7.148	2.380	1.730	1.308	0.219	0.0	1.44 (0.14)
	CrNbN	3.039	7.401	2.624	1.756	1.265	0.277	0.0	1.55 (0.10)
	CrTaN	3.017	7.407	2.656	1.740	1.273	0.334	0.0	1.67 (0.10)
DFT–PW91	CrVN[f]	2.86	7.14	2.313	1.763	1.300	0.158	0.0	···
	CrVN[g]	2.857	7.125	···	···	···	···	···	···
	CrNbN[g]	3.041	7.387	···	···	···	···	···	···
Experiment	Cr(V,Nb)N[h]	2.86	7.39	···	···	···	···	···	···
	CrNbN[i]	3.037	7.391	···	···	···	···	···	···
		3.029	7.360	2.576	1.730	1.324	0.350	···	···
	$Cr_{1.2}Ta_{0.8}N$[j]	3.004	7.334	···	···	···	···	···	···

[a]The lattice parameter a is for the MN compounds related to cubic nacl parameter d according to $d = \sqrt{2}a$.
[b]For the CrMN systems the Bader transfer from the Cr to the N atoms is also given in parentheses.
[c]DFT-PBE denotes results obtained in the current work.
[d]Experimental data from Ref. 41.
[e]Experimental data from Ref. 42.
[f]Theoretical data from Ref. 11.
[g]Theoretical data from Ref. 12.
[h]Experimental data from Ref. 4. The V:Nb atomic ratio is given as approximately 6:1.
[i]Experimental data from Refs. 36 and 35.
[j]Experimental data from Ref. 35.

and 12, whereas there are some discrepancies for the stated interlayer distances for the CrVN phase in Ref. 11. In an attempt to understand these deviations, we have repeated the bulk calculation for CrVN with the PW91 xc-functional. However, the obtained interlayer distances and cell parameters are within 0.005 Å identical to our PBE results, and hence, the different xc-functional cannot explain the discrepancies. Presumably, the differences can instead be attributed to the number of valence electrons utilized in the PAW potential for each element, the precise k-point grid, or the used energy cutoff. Neither is explicitly stated in Ref. 11.

Further, the atom-projected DOSs of the nitride phases are presented in Fig. 2. The nature of the chemical bonding in the MN compounds is well established and has been determined as a mixture of covalent, ionic, and metallic contributions. The contributions are associated with (i) the hybridization between the M and N atoms, leading to formation of bonding and antibonding pd states, (ii) the charge transfer from the M atom to the N atom, and (iii) the hybridization between the M atoms.[58–60] The formed electronic structure consists of (i) a lower valence band (LVB) below −15 eV with mainly N states, (ii) an upper valence band (UVB) between −10 eV to −4 eV with a mixture of bonding N and M states, and (iii) a conduction band (CB) above −4 eV containing antibonding and nonbonding states with mainly M character.

The DOSs for the CrMN phases are found to be similar to the electronic structure of the MN phases, where characteristics of the LVB, UVB, and CB are clearly visible. The main difference is a pronounced hybridization occurring between the Cr and M states above −4 eV, which modifies the antibonding states in the CB. Presumably, this beneficial Cr–M interaction is an important contributing factor to the higher stability of the CrMN phases compared to the MN compounds. Further, we find a presence of Cr states in the UVB between −9 to −4 eV, which supports formation of Cr–MN bonds. This interaction is also confirmed by the

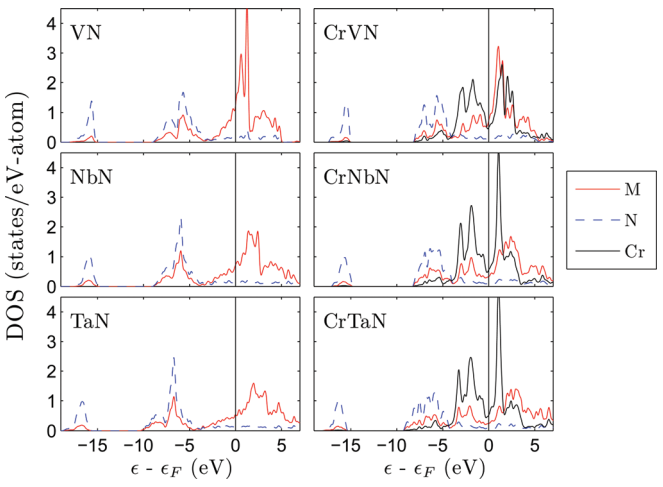

FIG. 2. (Color online) The atom-projected DOSs for the MN and CrMN bulk phases.

Bader analysis, which in addition to the charge transfer from the M to the N atoms also shows a charge transfer from the Cr atoms to the MN layers. All together, the bonding nature in the CrMN phases therefore comprise covalent, ionic, and metallic contributions as for the MN compounds, although with more weight on the metallic character.

B. Interface properties

In Table II we summarize the strains and the corresponding changes in the internal structural parameters for the coherently strained nitride bulk phases. Further, the calculated surface energies for the unstrained and strained phases are presented in Table III.

For the NbN and TaN compounds, we find that the misfit with respect to the iron lattice introduces very large strains, which cause a substantial decrease of the surface energies, and correspondingly, a reduction of the interlayer bonding along the *c*-axis. In contrast, the strains in the VN phase are much smaller and the effect on the interlayer bonding is less pronounced.

For the CrMN compounds, the strains are reduced compared to the MN phases due to a decreased misfit. Yet, the strains are not small for CrNbN and CrTaN. The lateral strain along the *c*-axis is found to arise primarily from an elongation of the interlayer distance c_{MM}, which suggests that the interaction between the MN layers is of less importance for the bond strength in the CrMN phase than the MN–Cr and Cr–Cr bonds. This weaker MN–MN interaction is confirmed by comparing the surface energies, which shows that the energy cost to create the $Z_{MN-Cr-Cr-MN}$ surface is much lower than the other two terminations. However, it is interesting to note that an accompanying enhanced internal buckling in the strained bulk phases leaves the interlayer distance between the nitrogen atoms, $c_{NN} = c_{MM} - 2c_{MN}$, nearly unchanged as compared to the unstrained compounds.

1. Chemical contribution

The calculated chemical contribution to the total interface energy and the work of separation for the Fe|MN and Fe|CrMN interface systems are presented in Fig. 3 as a function of the number of layers. Further, the corresponding converged values are summarized in Table III.

For the Fe|MN interface systems, the chemical contributions show a rapid convergence with respect to the number of layers, with deviations occurring mainly for the first one or two layer(s). The converged values are found to be negative, and consequently, the interface bonds are stronger than the average bond strength of the corresponding bulk phases. This beneficial interaction has, in previous theoretical studies, been shown to be due to strong Fe–N and Fe–M hybridization comprising aspects of ionic, covalent, and metallic character similar to the bonds in the bulk MN systems.[18,21,25,34]

For the Fe|CrMN interfaces, the chemical contributions are found to be well converged at four layers. The $Z_{MN-Cr-Cr-MN}$ layer ordering is determined to be the least energetically favorable termination for all three M-containing systems, whereas the $Z_{MN-MN-Cr-Cr}$ geometry is the optimal configuration for the Fe|CrNbN and Fe|CrTaN interfaces. In contrast, for the Fe|CrVN system the $Z_{Cr-MN-MN-Cr}$ layer ordering yields the lowest chemical contribution to the interface energy.

Further, examination of the work of separations reveals that even though the interface energies are positive, the Fe|CrMN interface bonds are still strong. In particular, the bonds at the Fe$|Z_{Cr-MN-MN-Cr}$ and Fe$|Z_{Cr-MN-MN-Cr}$ interfaces are stronger than the bonds at the Fe|MN interface, and the intrinsic bond strength in bulk Fe ($\bar{W}_{sep} = 5.0$ J/m^2). In fact, the interactions at the Fe$|Z_{Cr-MN-MN-Cr}$ interface are also even stronger than previous theoretical results for the work of separation for the Fe(001)|Cr(001) interface ($W_{sep} = 5.37$ J/m^2),[61] and the intrinsic bond strength for the (001) layers in bcc Cr ($\bar{W}_{sep} = 6.48$ J/m^2).[62] Meanwhile, the Fe$|Z_{MN-Cr-Cr-MN}$ interface is determined to be weaker than the Fe|MN interface, but stronger than the MN–MN interactions in the nitride phases.

2. Elastic contribution

The elastic contribution per layer to the total interface energy is presented in Table III. For the Fe|VN and Fe|CrVN interfaces, the energy costs for the coherency strains are found to be small, which suggests a possibility that thin coherent films of several layers can be stabilized in the Fe phase. For the Fe|VN system, this result is consistent with experimental observations of thin coherent VN platelets in Fe.[17,63] In contrast, for the Fe|NbN and Fe|TaN interfaces the elastic contributions are substantially larger, and the presence of coherent films thicker than one or two layers would be very unfavorable. Instead a transition to a semicoherent structure is to be expected.[34] Meanwhile, for the Fe|CrNbN and Fe|CrTaN interfaces, the elastic costs are

TABLE II. Calculated parallel and perpendicular strains ($\epsilon_{\parallel}$, $\epsilon_{\perp}$), induced changes in the interlayer distances between planes consisting of A and B atoms (Δc_{AB}), magnetic moments (m), and Bader charge transfer from the M to the N atoms (Bader) for the coherently strained bulk nitrides.

System	$\epsilon_{\parallel}$ (%)	$\epsilon_{\perp}$ (%)	Δc_{MM} (Å)	Δc_{MCr} (Å)	Δc_{CrCr} (Å)	Δc_{MN} (Å)	m (μ_B)	Bader ($\lvert e\rvert$)[a]
VN	−2.69	1.53	0.031	—	—	—	0.0	1.61
NbN	−9.92	11.40	0.254	—	—	—	0.0	1.72
TaN	−9.31	13.53	0.300	—	—	—	0.0	1.94
CrVN	−0.82	0.60	0.027	−0.002	0.019	0.011	0.0	1.45 (0.13)
CrNbN	−6.60	5.30	0.298	0.020	0.056	0.170	0.0	1.55 (0.04)
CrTaN	−5.92	4.73	0.243	0.031	0.045	0.116	0.0	1.68 (0.04)

[a]For the CrMN systems the Bader transfer from the Cr to the N atoms is also given in parentheses.

TABLE III. Calculated strained (unstrained) surface energies for the nitrides (σ), work of separations (W_{sep}), and chemical and elastic contributions to the interface energy (E_{chem}, E_{el}) for the investigated systems. The surface energy for the Fe phase is $\sigma_{Fe} = 2.50$ J/m^2. The E_{el} contributions are for the CrMN phases given as an average cost per layer.

System	σ (J/m^2)	W_{sep} (J/m^2)	E_{chem} (J/m^2)	E_{el} (J/m^2-layer)
Fe|VN	1.11 (1.37)	3.64	–0.03	0.05
Fe|NbN	0.53 (1.87)	3.58	–0.55	1.33
Fe|TaN	0.52 (1.93)	3.74	–0.72	1.18
Fe|CrVN				
$-Z_{MN-MN-Cr-Cr}$	2.75 (2.77)	4.93	0.32	0.005
$-Z_{MN-Cr-Cr-MN}$	0.89 (0.96)	2.64	0.75	0.005
$-Z_{Cr-MN-MN-Cr}$	4.49 (4.57)	6.79	0.20	0.005
Fe|CrNbN				
$-Z_{MN-MN-Cr-Cr}$	3.11 (3.49)	5.58	0.03	0.40
$-Z_{MN-Cr-Cr-MN}$	0.43 (0.99)	2.04	0.89	0.40
$-Z_{MN-Cr-Cr-MN}$	4.73 (5.30)	6.86	0.37	0.40
Fe|CrTaN				
$-Z_{MN-MN-Cr-Cr}$	3.38 (3.84)	5.87	0.01	0.33
$-Z_{MN-Cr-Cr-MN}$	0.47 (1.02)	1.98	0.99	0.33
$-Z_{Cr-MN-MN-Cr}$	4.77 (5.31)	6.91	0.36	0.33

significantly lower than for the Fe|NbN and Fe|TaN systems, which could promote the formation of thicker films. However, the strains are not small and an extended investigation of the semicoherent structure would be required in order to determine the possibility of precipitation of thin coherent CrNbN and CrTaN films.

Finally, it should be mentioned that the very large strains, together with the mentioned pronounced effects on the surface energies in Sec. III B, raise a question about whether or not the utilized Baker–Nutting orientation relationships is a correct assumption for the Fe|NbN, Fe|TaN, Fe|CrNbN, and Fe|CrTaN interface systems. The differences between the calculated lattice parameters and experimental values contribute to this uncertainty as the elastic contributions are sensitive to the misfit. However, by using the experimental data for the lattice parameters the misfits are only lowered by 1%–2%, and hence, the strains still remain very large. Therefore, the possibility of other orientation relationships where the strains are smaller cannot be excluded.

V. DISCUSSION

A. Relaxation of the MN phase

The calculations of the interface energetics of the Fe|MN interfaces in this study have consistently been performed with no atomic relaxation for the MN phase due to the established dynamical instabilities along the X and K high symmetry points for the stoichiometric phase. In order to estimate the impact on the interface energetics from this constraint, we have performed additional calculations where the MN phase is allowed to relax according to a commensurate shear wave along the $[110]_{nacl}$ direction, corresponding to the instability at the K symmetry point. The obtained results for the bulk and interface properties are summarized in Tables IV and V, respectively.

For the unstrained MN bulk phases, the shear relaxation introduces a tetragonal distortion of the cell parameters, where the a parameter is reduced together with an elongation along the c-axis. The accompanying internal bucklings are interestingly found to be next to identical with the internal bucklings in the unstrained CrMN systems. It is therefore plausible that the internal bucklings in the CrMN compounds are directly inherited from the dynamical properties of the MN phases.

Further, the work of separation is found to increase for the Fe|VN interface, whereas it remains similar to the unrelaxed case for the Fe|NbN and Fe|TaN interfaces. Meanwhile, the elastic contribution to the interface energy per layer is reduced substantially for all systems. Therefore, the shear relaxation of the MN phases seems to promote formation of coherent films. However, a more elaborate investigation including vacancies and their influence on the structural relaxation must be undertaken in order to determine whether or not these results are applicable to the interface energetics of MN films.

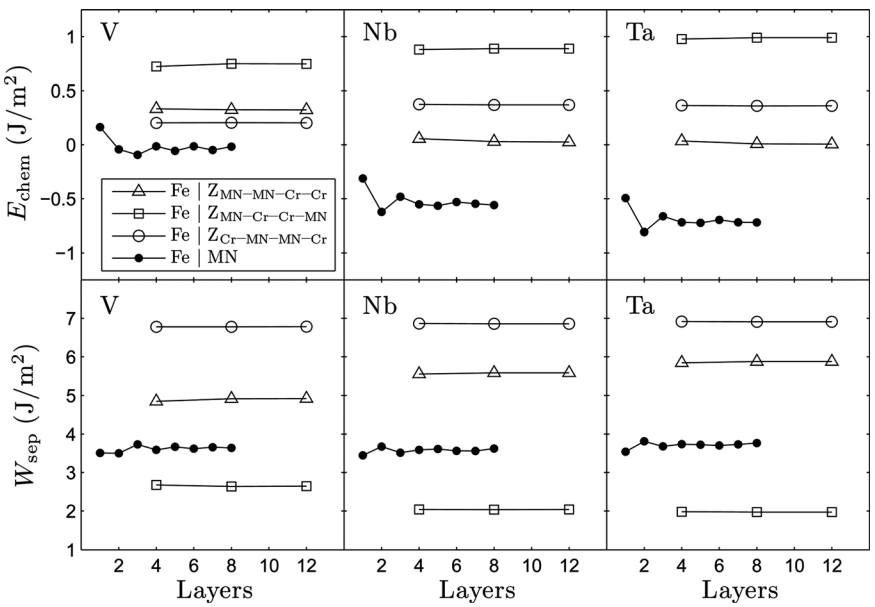

FIG. 3. The upper (lower) panels show the variations of the interface energy (work of separation) with respect to the number of nitride layers for the investigated Fe|MN and Fe|CrMN interfaces.

TABLE IV. Calculated lattice parameters (a, c), interlayer distances c_{AB} between planes consisting of A and B atoms, magnetic moments (m), and Bader charge transfer from the M to the N atoms (Bader) for the sheared MN bulk phases.[a]

System	a (Å)	c (Å)	c_{MM} (Å)	c_{MN} (Å)	m (μ_B)	Bader ($\|e\|$)
VN	2.888 (2.8385)	4.208 (4.291)	2.338 (2.451)	0.178 (0.235)	0.0 (0.0)	1.63 (1.62)
NbN	3.112 (2.8385)	4.561 (5.345)	2.562 (2.969)	0.267 (0.589)	0.0 (0.0)	1.71 (1.48)
TaN	3.069 (2.8385)	4.610 (5.324)	2.603 (3.257)	0.355 (0.529)	0.0 (0.0)	1.82 (1.62)

[a]The values when the phases are strained to coherency with the Fe lattice are also given in parentheses.

B. Stability of MN versus CrMN

The interface energetics of the MN and CrMN films has so far only been evaluated with respect to the corresponding stoichiometric bulk phases. Although such a procedure allows for a comparison between the MN and CrMN interface systems in terms of the work of separations and the elastic cost to the strain nitride phases, the total interface energy cannot be compared due to the choice of different chemical potentials. Consequently, our results alone cannot determine if the interface energies for the CrMN phases are higher than for the MN compounds, and by extension, whether or not the interface energy is the underlying reason behind the nucleation difficulty of the Z-phase in 9%–12%Cr steel alloys. For this purpose appropriate values for the chemical potentials would be required. However, the determination of the chemical potentials during the nucleation stage in a multicomponent alloy is a not an obvious procedure, as they depend on, e.g., the temperature and the concentrations of the elements. It would therefore be necessary to perform thermodynamical modeling of the alloys. Once completed, the acquired reference states can then be combined with our obtained results for interface energies in order to determine the possibility of direct Z-phase nucleation in the steel lattice.[64] However, such a treatment is beyond the scope of the present work and has been postponed for future work.

TABLE V. Calculated strained surface energies for the nitrides (σ), work of separations (W_{sep}), and chemical and elastic contributions to the interface energy (E_{chem},E_{el}) for the Fe|MN interface systems with a sheared MN phase.[a]

System/Layers	2	4	6	8
Fe|VN				
$-\sigma$	1.68	1.64	1.58	1.56
$-W_{sep}$	4.32	4.25	4.18	4.17
$-E_{chem}$	−0.14	−0.11	−0.11	−0.11
$-E_{el}$	0.04	0.08	0.12	0.16
Fe|NbN				
$-\sigma$	1.05	1.27	0.88	0.93
$-W_{sep}$	3.59	4.01	3.56	3.61
$-E_{chem}$	−0.04	−0.24	−0.19	−0.19
$-E_{el}$	1.02	2.04	3.06	4.08
Fe|TaN				
$-\sigma$	1.25	1.35	1.01	0.96
$-W_{sep}$	3.87	4.22	3.85	3.82
$-E_{chem}$	−0.12	−0.37	−0.35	−0.37
$-E_{el}$	0.38	0.76	1.14	1.52

[a]The surface energy for the Fe phase is $\sigma_{Fe} = 2.50$ J/m^2.

VI. CONCLUSIONS

In this work we perform a systematic investigation of the interface energetics of thin coherent nacl-structured MN and tetragonal CrMN films in bcc Fe (M = V, Nb, Ta) with the aim to improve the understanding of the difference in the nucleation pathway between MN and CrMN precipitates in 9%–12%Cr steel alloys. We employ *ab initio* DFT calculations and determine the strength of chemical interactions across the interfaces together with the elastic costs associated with the coherency strains.

The results show that the chemical interactions across the Fe|MN interfaces are stronger than the bonds in the corresponding bulk systems, which is consistent with previous theoretical studies.[18,21,34] In contrast, the bonds at the Fe|CrMN interfaces are found to be weaker than the bonds in the bulk counterparts. Yet, the chemical interactions at two out of three investigated Fe|CrMN interface terminations are significantly stronger than for the Fe|MN interfaces.

Further, the elastic cost for the coherency strains is found to be very small for the VN and CrVN compounds due to a small lattice misfit with respect to the Fe phase, which suggests a possibility of formation of thin coherent films. In contrast, the elastic contribution is determined to be significantly higher for the NbN and TaN phases, and coherent films thicker than one or two atomic layers would therefore be energetically unfavorable. Meanwhile, the elastic costs are found to be lower for the CrNbN and CrTaN compounds than for the NbN and TaN phases due to a reduced lattice misfit. The probability of thicker coherent films are therefore deduced to be higher in the former compared to the latter.

Finally, we investigate the impact on the interface energetics from introducing a shear relaxation in the MN phase, which is associated with a dynamical instability of the stoichiometric nacl-structured phase. We find that the shear relaxation gives rise to a substantial reduction ($>60\%$) of the elastic contribution to the interface energy as compared to the nacl-structure, which makes the elastic costs for the MN and CrMN phases comparable to each other. Meanwhile, the effects on the chemical interactions at the interface are determined to be smaller, where the strength of the Fe|VN system increases only marginally, whereas it remains next to constant for Fe|NbN and Fe|TaN interfaces. Effectively, the shear relaxation therefore seems to promote the formation of thicker coherent MN films than for the nacl-structured MN phase.

In conclusion, our findings provide important information about the differences and similarities of the interface energetics of MN and CrMN films in Fe. In particular, both

the strength of the interface bonds and the elastic energy cost for the coherency strains can differ significantly between the compounds. These differences give support to that the interface energetics can play a decisive role in the initial nucleation stage of MN and CrMN precipitates. However, in order to draw any definite conclusions, the elastic contribution must be in relation to the chemical contribution to the total interface energy. For this purpose appropriate values for the chemical potentials are required. Our obtained results should therefore in future work be combined with thermodynamical modeling,[8,11,12] before the impact of the interface energetics in the initial nucleation stage of MN and CrMN precipitates in 9%–12%Cr steels can be determined.

ACKNOWLEDGMENTS

This work was supported by the Swedish Foundation for Strategic Research (SSF). The allocations of computer resources at C3SE and the Swedish National Infrastructure for Computing (SNIC) are gratefully acknowledged. The authors wish to thank Hans-Olof Andrén, John Hald, and Hilmar Danielsen for valuable comments and discussion.

[1]J. Hald, in *Proceedings of the First International Conference on Super-High Strength Steels* (AIM and CSM, Rome, Italy, 2005).
[2]T. Fujita, K. Asakura, T. Sawada, T. Takamatsu, and Y. Otoguro, Metall. Trans. **12A**, 1071 (1981).
[3]J. Hald and L. Korcakova, ISIJ Int. **43**, 420 (2003).
[4]A. Strang and V. Vodarek, Mater. Sci. Technol. **12**, 552 (1996).
[5]H. K. Danielsen and J. Hald, Energy Mater. **1**, 49 (2006).
[6]F. Kurosawa, I. Taguchi, M. Tanino, and R. Matsumoto, J. Jpn. Inst. Metals **45**, 63 (1981).
[7]H. K. Danielsen and J. Hald, Scr. Mater. **60**, 811 (2009).
[8]H. K. Danielsen and J. Hald, CALPHAD **31**, 505 (2007).
[9]H. K. Danielsen and J. Hald, VGB PowerTech **5**, 68 (2009).
[10]L. Cipolla, H. K. Danielsen, D. Venditti, P. E. D. Nunzio, J. Hald, and M. A. J. Somers, Acta Mater. **58**, 669 (2010).
[11]P. Lazar, R. Podloucky, E. Kozeschnik, and J. Redinger, Phys. Rev. B **78**, 134202 (2008).
[12]C. Kocer, T. Abe, and A. Soon, Mater. Sci. Eng. A **505**, 1 (2009).
[13]H. K. Danielsen, J. Hald, F. B. Grumsen, and M. A. J. Somers, Metall. Mater. Trans. 37A, 2633 (2006).
[14]H. K. Danielsen and J. Hald, Mater. Sci. Eng. A **505**, 169 (2009).
[15]H. K. Danielsen, "Z-phase in 9-12%Cr Steels," Ph.D. thesis (DTU, Denmark, 2007).
[16]R. Agamennone, W. Blum, C. Gupta, and J. K. Chakravartty, Acta Mater. **54**, 3003 (2006).
[17]N. E. Vives Díaz, S. S. Hosmani, R. E. Schacherl, and E. J. Mittemeijer, Acta Mater. **56**, 4137 (2008).
[18]J. Hartford, Phys. Rev. B **61**, 2221 (2000).
[19]A. Arya and E. A. Carter, J. Chem. Phys. **118**, 8982 (2003).
[20]J.-H. Lee, T. Shishidou, Y.-J. Zhao, A. J. Freeman, and G. B. Olson, Philos. Mag. **85**, 3683 (2005).
[21]W.-S. Jung, S.-H. Chung, H.-P. Ha, and J.-Y. Byun, Modell. Simul. Mater. Sci. Eng. **14**, 479 (2006).
[22]S.-H. Chung, H.-P. Ha, W.-S. Jung, and J.-Y. Byun, ISIJ Int. **46**, 1523 (2006).
[23]D. F. Johnson and E. A. Carter, J. Phys. Chem. A **113**, 4367 (2009).
[24]S. V. Dudiy, J. Hartford, and B. I. Lundqvist, Phys. Rev. Lett. **85**, 1898 (2000).
[25]S. V. Dudiy and B. I. Lundqvist, Phys. Rev. B **64**, 045403 (2001).
[26]M. Christensen, S. Dudiy, and G. Wahnström, Phys. Rev. B **65**, 045408 (2002).
[27]S. A. E. Johansson, M. Christensen, and G. Wahnström, Phys. Rev. Lett. **95**, 226108 (2005).
[28]M. Christensen and G. Wahnström, Acta Mater. **52**, 2199 (2004).
[29]J. Hoekstra and M. Kohyama, Phys. Rev. B **57**, 2334 (1998).
[30]D. J. Siegel, L. G. Hector, and J. B. Adams, Phys. Rev. B **67**, 092105 (2003).
[31]L. M. Liu, S. Q. Wang, and H. Q. Ye, Acta Mater. **52**, 3681 (2004).
[32]R. Benedek, D. N. Seidman, and C. Woodward, J. Phys. Condens. Matter **14**, 2877 (2002).
[33]R. Benedek, D. N. Seidman, and C. Woodward, Interface Sci. **12**, 57 (2004).
[34]D. H. R. Fors and G. Wahnström, Phys. Rev. B **82**, 195410 (2010).
[35]P. Ettmayer, Monatsch. Chem. **102**, 858 (1971).
[36]D. H. Jack and K. H. Jack, J. Iron Steel Inst. **209**, 790 (1972).
[37]T. C. Bor, A. T. W. Kempen, F. D. Tichelaar, E. J. Mittemeijer, and E. van der Giessen, Philos. Mag. A **82**, 971 (2002).
[38]F. Danoix, E. Bémont, P. Maugis, and D. Blavette, Adv. Eng. Mater. **8**, 2006 (2006).
[39]M. Perez, E. Courtois, D. Acevedo, T. Epicier, and P. Maugis, Philos. Mag. Lett. **87**, 645 (2007).
[40]V. Vodarek and A. Strang, J. Phys. IV France **112**, 445 (2003).
[41]H. O. Pierson, Handbook of Refractory Carbides and Nitrides (William Andrew/Noyes, Park Reidge, NJ, 1996).
[42]X.-J. Chen, V. V Struzhkin, Z. Wu, M. Somayazulu, J. Qian, S. Kung, A. N. Christensen,Y. Zhao, R. E. Cohen, H. Mao, and R. J. Hemley, Proc. Natl. Acad. Sci. U.S.A. **102**, 3198 (2005).
[43]G. Kresse and J. Hafner, Phys. Rev. B **47**, 558 (1993); **49**, 14251 (1994).
[44]G. Kresse and J. Furthmüller, Comput. Mater. Sci. **6**, 15 (1996).
[45]G. Kresse and J. Furthmüller, Phys. Rev. B **54**, 11169 (1996).
[46]G. Kresse and D. Joubert, Phys. Rev. B **59**, 1758 (1999).
[47]D. J. Singh, W. E. Pickett, and H. Krakauer, Phys. Rev. B **43**, 11628 (1991).
[48]J. P. Perdew, K. Burke, and M. Ernzerhof, Phys. Rev. Lett. **77**, 3865 (1996).
[49]M. Ropo, K. Kokko, and L. Vitos, Phys. Rev. B **77**, 195445 (2008).
[50]P. Haas, F. Tran, and P. Blaha, Phys. Rev. B **79**, 085104 (2009).
[51]R. F. W. Bader, Chem. Rev. **91**, 893 (1991).
[52]G. Henkelman, A. Arnaldsson, and H. Jònsson, Comp. Mater. Sci. **36**, 354 (2006).
[53]W. Tang and G. Henkelman, "DOS Projection in Bader Volumes (2010)," extended information about the tool can be found at http://theory.cm.utexas.edu/vtsttools/dos/.
[54]W. Weber, P. Roedhammer, L. Pintschovius, W. Reichardt, F. Gompf, and A. N. Christensen, Phys. Rev. Lett. **43**, 868 (1979).
[55]E. I. Isaev, S. I. Simak, I. A. Abrikosov, R. Ahuja, Yu. Kh. Vekilov, M. I. Katsnelson, A. I. Lichtenstein, and B. Johansson, J. Appl. Phys. **101**, 123519 (2007).
[56]V. I. Ivashchenko, P. E. A. Turchi, and E. I. Olifan, Phys. Rev. B **82**, 054109 (2010).
[57]J. P. Perdew, J. A. Chevary, S. H. Vosko, K. A. Jackson, M. R. Pederson, D. J. Singh, and C. fiolhais, Phys. Rev. B **46**, 6671 (1992).
[58]A. Neckel, P. Rastl, R. Eibler, P. Weinberger, and K. Schwarz, J. Chem. C: Solid State Phys. **9**, 579 (1976).
[59]C. D. Gelatt, A. R. Williams, and V. L. Moruzzi, Phys. Rev. B **27**, 2005 (1983).
[60]J. Häglund, A. F. Guillermet, G. Grimvall, and M. Körling, Phys. Rev. B **48**, 11685 (1993).
[61]D. F. Johnson, D. E. Jiang, and E. A. Carter, Surf. Sci. **601**, 699 (2007).
[62]T. Ossowski and A. Kiejna, Surf. Sci. **602**, 517 (2008).
[63]D. H. R. Fors, S. A. E. Johansson, M. Petisme, and G. Wahnström, Comput. Mater. Sci. **50**, 550 (2010).
[64]S. A. E. Johansson and G. Wahnström, Philos. Mag. Lett. **90**, 599 (2010).